Reactive Scheduling of Computational Resources in Control Systems

Gera Weiss
Ben-Gurion University
Beer-Sheva, Israel
geraw@cs.bgu.ac.il

Hodai Goldman
Ben-Gurion University
Beer-Sheva, Israel
hodaig@cs.bgu.ac.il

ABSTRACT

We present an approach to reactive scheduling of computations in software control systems. The main motivation comes form the growing use of computer vision algorithms in real-time, as sensors. The term reactive here refers to the ability of the scheduler to adapt the schedules dynamically based on physical conditions. We propose an extension of the automata based scheduling approach with an addition of guards to transitions that allow for reactive specifications. We develop a methodology for using Klman filters to provide data that guides these automata, and demonstrate the combined approach in simulations and with a case study. The case study is a development of a software that stabilizes a quadcopter in front of a window using a vision based sensor with a time-varying resolution, i.e., computation load is controlled by taking images in reduced resolution when the state of the controlled loop allows.

1. INTRODUCTION

Cyber-physical systems (CPS) technologies of integrating software and control are at the heart of many critical applications (c.f. [15]). These technologies aim at handling issues that emerge when the interaction of software and hardware brakes the traditional abstraction layers: when researchers and practitioners are required to consider a unified view that includes both software and hardware. An example of such an issue is the challenge of dynamic assignment of computational resources to software based controllers discussed in, e.g., [3, 22, 24]. While the computation burden required by the control loops can be ignored in many situations, this is not always the case. A main motivating example studied in this paper is vision based control, where computer vision algorithms acquire state information to be used in a feedback loop (c.f. [7, 9, 20]). Unlike conventional sensors such as accelerometers, gyros, compasses, etc., a visual sensor requires significant processing of the acquired image to prepare the state information for feedback. Since typical cyber-physical application, such as robot control, consist of many control loops, responsible for different aspects of the system, that run simultaneously and share the same computational resources, computer vision algorithms cannot always be invoked in full power. Alternatively, we propose in this paper a mechanism to dynamically trade CPU consumption vs. measurement accuracy so that data acquisition algorithms run in full power only when the control loop requires accurate data.

A main challenge in forming mechanisms for the integration of software and control lies in the design of efficient interfaces for integrating the engineering diciplines involved (c.f. [24]). Components with clearly specified APIs, such as Java library classes, allow designers to build complex systems effectively in many application domains. The key to such modular development is that an individual component can be designed, analyzed, and tested without the knowledge of other components or the underlying computing platform. When the system contains components with real-time requirements, the notion of an interface must include the requirements regarding resources, and existing programming languages provide little support for this. Consequently, current development of real-time embedded software requires significant low-level manual effort for debugging and component assembly (cf. [11, 14, 19]). This has motivated researchers to develop compositional approaches and interface notions for real-time scheduling (cf. [5, 6, 8, 16–18, 21, 23]).

In this paper we present an approach, a proof-of-concept implementation, and a case study in scheduling computations in embedded control systems. The proposed design is based on the automata based schedul-

ing approach, suggested in [1, 2, 25], where automata are proposed as interfaces that allow the dynamicity and efficiency of desktop operating systems with the predictability of real-time operating systems. The approach allows for components to specify the CPU resources that they need in a way that gives an application agnostic scheduler the freedom to choose schedules at run-time such that the needs of all the components are taken into account, even of components that were added only at run-time. The main contributions of this paper relative to the earlier work in this direction is: (1) We propose an extension of the automata based scheduling frame work that allows to direct the schedule based on the state of the controllers; (2) We propose a technique, based on the theory of Kalman Filters, for designing reactively scheduled controllers; (3) We report on our experience with improving the performance of a real-time, vision-based, control system (a quadrotor that stabilizes itself in front of a window).

The rest of the paper is organized as follows: In Section 2 we outline the general software approach and the methodologies developed in our research. In Section 3 we present the technical details of the proposed approach using a simulation. The case study is presented in Section 4 with a description of the engineering setup and the data we collected for the evaluation of the approach.

2. THE PROPOSED APPROACH

As proposed in earlier work on automata based scheduling (cf. [1,2,25]) we aim at a development process where a system is built as a composition of a set of components where each component is a aoftware module (a set of procedures) accompanied with an automaton. Our addition here is that we allow the automata to be guarded, i.e., each automaton acts as a specification of a reactive system that tells the scheduler which functions of a component it may run in each slot depending on the dynamic state of the controllers. A second addition is that we have implemented the approach as an enhancement of the internal scheduler of the ArduPilot Mega (APM) open source unmanned vehicle autopilot software suite (`http://www.ardupilot.co.uk/`). A third contribution of the paper is a proposal of a specific way to use the automata based scheduling framework with a Kalman filter. We elaborate on each of these in the following subsections:

2.1 Guarded Automata as Interfaces for Control and Scheduling

As our goal is to allow dynamic selection of the computation load in the feedback loops based on the states of the systems, we start with a general software architecture in which each component (implementation of a feedback specific loop) is represented by a code module (in our case, a class in C++) and an automaton that specifies when to invoke its methods. The transition relation of the automaton depends, in addition to the current state, also on a real number produced by the estimator of the feedback loop (we experimented with different options for this number, as discussed below).

The motivations of using automata as described above are: (1) Automata allow for a rich specification language; (2) It is easy to construct schedules that obey the specification with negligible computational burden; (3) Automata theory gives a solid framework for composing the specifications of competing requirements for analysis and for schedule synthesis.

In this paper we focus on the first two motivations in the above list. The third is discussed in details in earlier paper on automata based scheduling (cf. [1,2,25]) and is the focus of another paper that we are preparing where we describe some analysis techniques we have developed for guarded automata.

2.2 Implementation in an Auto Pilot Software

As our main case study is in flight control, we chose the ArduPilot Mega (APM) platform for experiments. To this end, we implemented a basic automata based scheduler for this platform. The built-in task scheduling specification in APM consist of a table as shown in Figure 1. This table is easy to maintain and to use, but it is used under an assumption that there is enough CPU power to run all the tasks in the specified frequencies. APM does contain a mechanism to handle overruns, by moving tasks to the next window when there is not enough time to run them now, but the system is designed under the assumption that this only happen in rare situations.

To allow a reactive schedule that runs different modes of the software-based controllers depending on their state, we replaced the scheduling table in our version of the APM with automata that specify when to run the tasks. Note that automata allow for specifying the requirements that the table represents, using simple circular automata without guards (see, e.g., [24]). Automata, however, can model more advanced scheduling instructions with very little addition to the complexity of the scheduler, as we will demonstrate in Section 3 and in Section 4 below.

2.3 Integration With a Kalman Filter

The third layer of the approach we propose is based on the observation that a standard Kalman filter produces information that can be used to guide the automata of the components.

As we will elaborate in the description of the simulations and of the case study below, we propose to sched-

```
/*
  scheduler table - all regular tasks apart from
  the fast_loop() should be listed here, along
  with how often they should be called (in 10ms
  units) and the maximum time they are expected
  to take (in microseconds)
*/
static const AP_Scheduler::Task
     scheduler_tasks[] PROGMEM = {
        { update_GPS,             2,     900 },
        { update_nav_mode,        1,     400 },
        { medium_loop,            2,     700 },
        { update_altitude,       10,    1000 },
        { fifty_hz_loop,          2,     950 },
        { run_nav_updates,       10,     800 },
        { slow_loop,             10,     500 },
        { gcs_check_input,        2,     700 },
        { gcs_send_heartbeat,   100,     700 },
        { gcs_data_stream_send,   2,    1500 },
        { gcs_send_deferred,      2,    1200 },
        { compass_accumulate,     2,     700 },
        { barometer_accumulate,   2,     900 },
        { super_slow_loop,      100,    1100 },
        { perf_update,         1000,     500 }
};
```

Figure 1: APM scheduling specification

ule the functions that implement algorithms for sensing and for actuation based on the variance of the estimation that a Kalman filter provides.

3. A DEMONSTRATION OF THE APPROACH IN SIMULATION

Our approach for using automata for scheduling resources in software based controllers is based on the observation that in most systems the computational load is in the implementation of the sensors and of the actuators, not in the implementation of the controllers that usually consist of quick arithmetic manipulation of a small amount of variables. We therefore focus our attention on allowing a trade-off between CPU usage of sensors and actuators and their accuracy.

Formally, we assume that the physical system we control is a Linear Time Invariant (LTI) system with a known model, as depicted in Figure 2. The inaccuracies of the sensors and of the actuators are modeled as additive Gaussian noise with a known variance. As a basis for scheduling, we assume that each sensor can be scheduled to operate in one of a range of modes at each computation slot, each mode consuming a certain percentage of the CPU and giving a certain variance of the measurement noise.

The scheduling of the modes is governed by the automata based scheduler as depicted in Figure 2. We propose to use a standard Kalman filter as a tool to gather the information that guides the state evolution of the automata, as follows. The filter gets as input the actuations, measurements, and the variance of the measurement noise, which we assume is a function of the

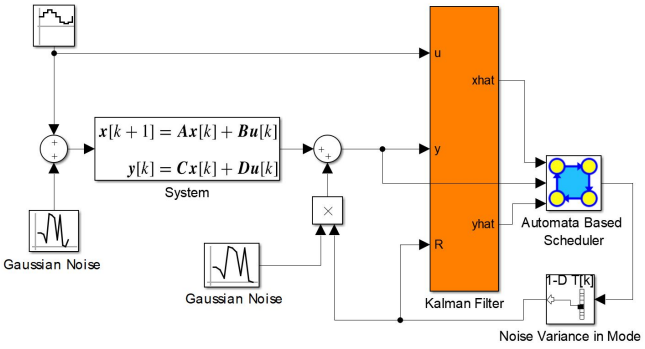

Figure 2: A Simulink model demonstrating the proposed approach.

sensor mode chosen by the scheduler. The output of the Kalman filter is fed to the scheduler that uses it for controlling the modes of the sensor. In the Simulink model depicted in Figure 2, the scheduler feeds the variance of the disturbance to the Kalman filter and to the block that multiplies the noise by the variance (the product of a white noise with unit variance and a constant C yields a normally distributed noise with variance C).

We ran the model depicted in Figure 2 with the linear time invariant system:

$$\begin{aligned} x(k+1) &= \begin{pmatrix} 1.3 & -0.5 & 0.1 \\ 1 & 0 & 0 \\ 0 & 1 & 0 \end{pmatrix} x(k) + \begin{pmatrix} -0.4 \\ 0.6 \\ 0.5 \end{pmatrix} u(k) \\ y(k) &= \begin{pmatrix} 1 & 0 & 0 \end{pmatrix} x(k) \end{aligned}$$

taken from `https://www.mathworks.com/help/control/examples/kalman-filter-design.html`. As seen in Figure 2, we injected a sinusoidal input (with $amplitude = bias = frequence = 1$) to this system. The actuation noise, depicted on the left, is with a unit variance.

The 'Automata Based Scheduler' block is designed to set the variance of the sensing noise dynamically to be either 0.25 or 1 at each step of the simulation. This models a sensor that has two modes of operation: a mode with high accuracy that produces noise with low variance and a mode with low accuracy that produces errors with higher variance. We assume, for the performance measurements presented below, that the CPU consumption of each mode is $\%CPU = 1.1 - errVar$, where $errVar$ is the variance of measurement error in the mode.

We ran this models with three versions of the 'Automata Based Scheduler' block. The first version, called 'High' in Table 1, is where the block acts simply as the constant 1, ignoring its inputs altogether. Similarly, the term 'Low' in the table refers to an implementation where the block is the constant 0.25. These two implementations model the constant schedules, where

	High	Low	Aut. Based
%CPU	0.85	0.1	0.46
mean of $\|x - \hat{x}\|$	0.97	1.24	1.08

Table 1: Simulation results.

the sensor is operated in one mode along the whole execution. These two schedules are compared to a third implementation, called 'Automaton' in the table, where the block implements the schedule given by the automaton:

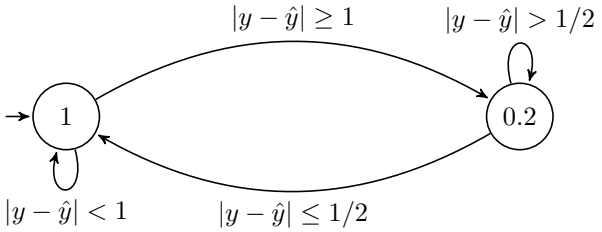

where the name of a state defines the variance of the estimation noise when entering it.

The results of the simulation, summarized in Table 1, show, as expected, that the CPU consumption is much lower (0.1) when using the low-quality version of the sensing algorithm and is higher (0.85) when the high-quality version of the sensing algorithm is used. The performance of the estimation in terms of the mean distance between x and $\hat{x}$ better with the high-quality version (0.97) than it is with the low-quality version (1.24). More interestingly, we can see that the experiment with the automaton that switches between the two sensor modes yields performance that is close to the performance of the high-quality sensing algorithm, using much less CPU.

4. CASE STUDY: STABILIZING A QUADROTOR IN FRONT OF A WINDOW

The case study we used to test our concept is the development of a controller that stabilizes a quadrotor [**?**] in front of a window. We implement an autonomous controller for that task and evaluated its performance.

The part of the controller that we focused on is the vision based position controller. Specifically, the main controller, that we will describe below, uses a standard low-level angular controller and a simple image processing algorithm that identifies the position of the corners of the window in the image plane[1]. Its goal is to regulate the position of the quadrotor by tilting it. Note that rotations of the quadrotor generate a more-or-less proportional accelerations in a corresponding direction. A main challenge for this controller is that the computer vision algorithm takes significant time to compute relative to the fast control loop. We can decrease computation time by lowering the resolution, but this also increase the measurement noise. We will demonstrate how adaptive scheduling of the resolution can serve for balancing resource consumption vs. control performance.

4.1 Observer Design

We first implemented an observer based on the work of Efraim at al. [**?**]. The observer gets the positions of the widow corners, enumerated clockwise starting from the top left corner noted by p_1, p_2, p_3, p_4, and extract 4 quantities based on the shape and location of the window corners in the image plane: S_x , s_y , V_d and sz. **center of mass:** S_x and S_y represent the window "center of mass" in the image plane along the image x and y axes, respectively. S_x and S_y are normalized to the range of $[-1, 1]$. S_x is used to measure the roll angle of the window center (for stabilize the roll axis), and S_y is used to measure the altitude of the drone (for stabilizing the throttle). **Window size:** sz is the sum of the vertical edges of the window, sz is used to measure the distance of the drone from the window and then to regulate the roll angle [2]. **Vertical difference:** $V_d = \frac{y_1 - y_4 - (y_2 - y_3)}{y_1 - y_4 + (y_2 - y_3)}$, were y_i is the vertical position of p_i in the range of $[-1, 1]$ (0 is the center of the image) first is used to measure the angular position of the drone in relation to the window (θ), then θ and sz are used to calculate the horizontal position parallel to the window surface (x position) of the drone (see Figure 3).

REMARK 1. *We assume that process state (x) is governed by the linear [3] stochastic difference equation:*

$$x_k = Ax_{k-1} + Bu_k + w_k$$

And the measurement (z_k) at time k is:

$$z_k = Cx_k + v_k$$

The random variables w_k and v_k represent the process and measurement noise (respectively).

After measuring the relative position and yaw attitude, as usual, we add estimator filter to get better state estimation. In theory, and s shown in the simulation at Section 3, we should use Kalman filter estimator for best state estimation, in our case is non-linear system and the process noise distribution is problematic to determine (battery state affects the system dynamics), this with the complexity of kalman filter lead us

[1] In the experiment, to simplify the image processing algorithm, we marked the corners of the window with led lights.

[2] we use fixed size window and convert sz to distance (in meter in our case) based on this window, in the general case the distance is relative to the window size

[3] we make approximation of our non-linear system by linear difference equation

simplify the kalman filter principles using complementary filter, a simple estimation technique that is often used in the flight control industry. Complementary filter is actually a steady-state Kalman filter for a certain class of filtering problems [13]. We use two steps estimator that, (1) *predict* the current state evolved from the previous state using a linearized model of the system ($x_{k|\hat{k}-1}$) and then *update* the prediction with current state measurement from image, noted by z_k. The result estimation (noted by $\hat{x}_{k|k}$) is a complementary filter of the prediction ($\hat{x}_{k|k-1}$) and the measured state ($C^{-1}z_k$): $\hat{x}_{k|k} = K\hat{x}_{k|k-1} + (1-K)C^{-1}z_k$ were K is constant approximation of the kalman filter gain (K_k).

The image processing have few different operation modes, every mode has different accuracy (shown in Section 4.3). Similarly to the gain of kalman filter, K represent the ratio between process noise and measurement noise distribution, therefore K is defined separately for each mode to achieve the best estimation in each mode.

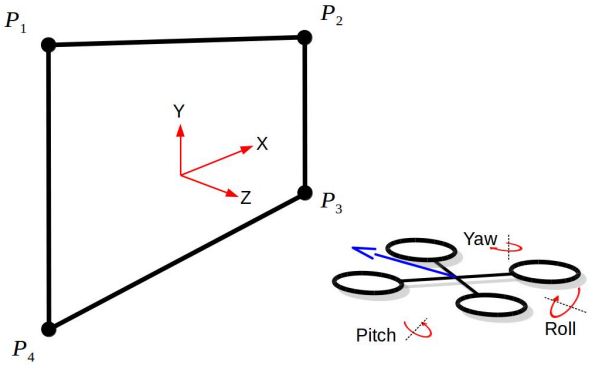

Figure 3: Description of Coordinate System and Rotation Axis.

4.2 Controller Design

In this experiment, we consider the task of *hovering in front of the window*, the controller objective is to hover parallel to the window (center of x axis) at the altitude of the window within distance of 2 meters in front of the window and face pointed to the center of the window (yaw angle). We consider this point as the origin and the coordinates are according to Fig. 3.

The controller consist of 4 independent feedback control loops, altitude, yaw angel, pitch and roll. Pitch and roll controllers composed from, low level attitude controller which his input is the required pitch or roll angel accordingly, and high level position controller which his input is the required distance or x position relative to the window accordingly, the high level controller outputs the required angle (acceleration) to the low level controller as show in Fig. 4. All the loops control regulate the position or attitude relative to the window. The inertial (angular) feedback is generated by the existing *Attitude and heading reference system* (AHRS) library of ArduPilot see Section 5, and the window related feedback come directly from the observer described in Section 4.1.

Based on the separation principle, we can use that controller regardless the measurement quality, in practice we implement basic Proportional Integral Derivative (PID [4]) controller and tuned the parameters with the highest resolution observer.

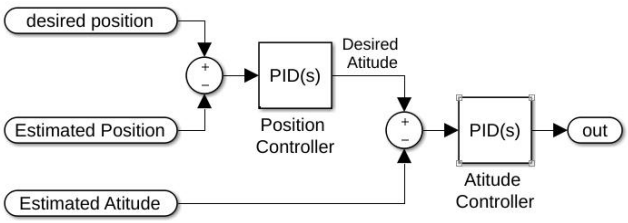

Figure 4: Atitude and Position Controller - Two level structure

4.3 Analysis and Specification Automata

The objective of the system is to maintain stable hovering in front of the window. Hence, the performances of the system is measured by the amount of deviation from the center line of the window in the critical axis x, meaning, we want to minimize $|x|$ (see Figure 3). Our goal is to achieve maximum performance with minimal amount of processing time. Obviously, both goals can not be achieved together, the task is to set the best trade-off between them. The problem comes from the main consumer of computation resources, the image-based observation tasks. In this part, we use different observation modes together in order to improve the resource utilization, meaning we use more resources (CPU time) only when it is needed, and this way reduce the overall CPU usage without significantly affect the performance. In fact, we switch the camera resolution during the flight, the image resolution define the operation mode (see Section 4.1). For simplicity, in this work we examine only two modes, *High quality* with resolution of 960p and *Low quality* with resolution of 240p.

Analyzing the test results shown in Table 2, we see that High quality observation mode provide mean (x) error tolerance of 9.5 *cm* [4], and with the cost of 30% CPU usage. On the other hand, Low quality mode provide worse mean error of co *cm* (three times High quality mode), but cost only 2.1% CPU usage [5]. In this section we show how defining *adaptive scheduling*

[4]All lengths are measured in Centimeter.

[5]The CPU usage percentage is the average usage, and is calculates as $\frac{\text{total time spend in image processing}}{\text{total flight time}}$.

specification in order to lower the CPU usage without significant worsening of High quality performances.

First we examine a straight-forward solution based directly on the current position (the x part of $\hat{x}_{k|k}$). Using the simple guard automaton A_x presented in Fig. 5, we define dynamic observer that choose the operation mode (high or low quality) based on the x part of $\hat{x}_{k|k}$ absolute value, if the drone is closer to the center line of the window, noted by $|x| < T_x$, we consider it as "safe" state and go to L mode that use the low quality image. Similarly, "BAD" states are when the drone is far, noted by $|x| > T_x$, then we use High quality image in order to "fix" the bad state. The trash-hold T_x value can be changed to define the desire performances and processing time trade-off. Results shows good improvement in term of resource utilization (see Section 4.4).

DEFINITION 1. *Measurement post-fit residual $\tilde{y}_{k|k}$, is the difference between the expected measurement ($C \cdot \hat{x}_{k|k}$) and the measured state (z_k): $\tilde{y}_{k|k} = |\hat{x}_{k|k} - z_k|$* [6].

From the Low quality experiment graph we can see that $\tilde{y}_{k|k}$ accumulates proportional to the deviation from the center of x axis, we can use $\tilde{y}_{k|k}$ vales to predict high deviation from x. In the second experiments set we used A_{err} Automaton presented in Fig. 5, which is similar to A_x but switch states based on $\tilde{y}_{k|k}$ value. In this case the observer operate in low quality when $\tilde{y}_{k|k} < \alpha_{low}$ ("GOOD" state), and change to high quality when $\tilde{y}_{k|k} > \alpha_{high}$ ("BAD" state). The trash holds values α_{low} and α_{high} has determined first from the low and high quality graph and fine tuned by experiments. Different α_{low} and α_{high} achieve different trade-offs of performances and processing time. Note, in Section 4.4 we show how this dynamic observer do not result significant affect to the performance but reduce by factor of $\frac{1}{2}$ the processing time.

The expressiveness of Automata allows creating even more complex task specification, we can for example combine the approaches of both A_{err} and A_x. In Fig. 5 there is two examples of such combination, A_{comp1} try to save unnecessary CPU usage while the drone is in "safe" state, close to the center, and activate A_{err} only if the drone gone far from the center (T_x cm from the origin). A_{comp2} add another constrain that if the drone gone even farther away (T_{x2} cm from the origin) use only high resolution to bring it back to safety. The result shows even greater resource utilization.

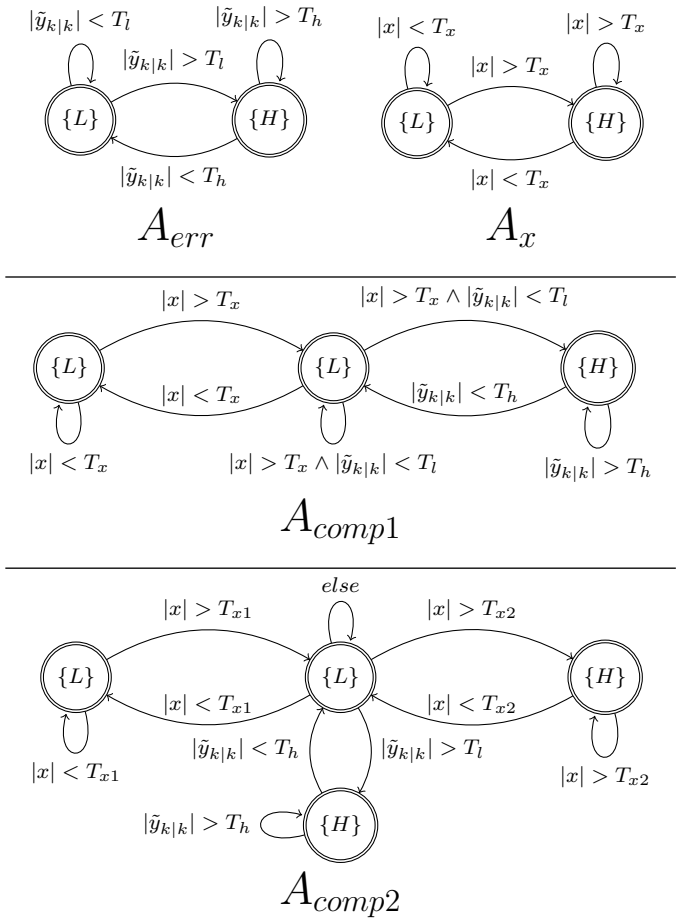

Figure 5: The main Automata we used for describing the specifications in the experiments.
A_{err} uses the *measurement post-fit residual* ($\tilde{y}_{k|k}$), if $|\tilde{y}_{k|k}|$ is too small then next iteration will use small resolution image (L), and if too large the high resolution will be used, T_l and T_h are the transition trash-holds.
A_x operate similar to A_{err} but uses the current position (the x part of $\hat{x}_{k|k}$) instead $\tilde{y}_{k|k}$, with the trash-hold T_x.
A_{comp1} and A_{comp2} are the results of composing the A_{err} and A_x ideas.

4.4 Results

Table 2 summarize the result of flight experiments made using the specification Automata describing in

[6]Measurement post-fit residual $\tilde{y}_{k|k}$ is also defined by Kalman filter

Section 4.3. The first column "% CPU" represent processing time usage by image processing task, and is calculates as $\frac{\text{total time spend in image processing}}{\text{total flight time}}$. The second column *mean*(|x|)" is the average distance of the drone from the origin in the x coordinate, the real x position of the drone is monitored using *OptiTrack* system (see Section 5) and presented in centimeter units. All the statistics shoen in the table are from real indoor experiment flights of between 1 to 2 minutes.

Table 2: Test Results

Schedule	**% CPU**	**mean($\|x\|$) (cm)**	**max($\|x\|$) (cm)**
Only High	30.9%	9.5	31.2
Only Low	2.1%	30.0	70.9
A_x ($T_x = 10$)	16.6%	10.9	42.5
A_x ($T_x = 20$)	14.0%	14.1	**32.1**
A_x ($T_x = 30$)	8.9%	17.4	**48.4**
A_{err} ($T_l = 10, T_h = 20$)	10.3%	14.9	43.2
A_{err} ($T_l = 10$, $T_h = 15$)	11.7%	11.3	36.3
A_{comp1} ($T_x = 10$, $T_l = 10$, $T_h = 15$)	8.8%	12.9	32.1
A_{comp2} ($T_{x1} = 10$, $T_{x2} = 30$, $T_l = 10$, $T_h = 15$)	10.4%	12.7	36.6

5. EXPERIMENT SETUP

In order to perform the experiments we used of-the-shelf quad rotor with *navio2* [**?**] and *Raspberry pi* [**?**] flight controller that runs a modified *ArduPilotMega-arducopter* [**?**] software. *Navio2* is extension board (shield) for the *Raspberry pi* [**?**] platform, it provides the nessesary interfaces such as remote control inputs and motors output, and it's equipped with 3-axes gyroscop and accelerometer MEMS sensors [**?**]. We used the standard raspberry pi camera.

6. CONCLUSIONS

Conclusion goes here.

Acknowledgments

Acknowledgement goes here.

7. REFERENCES

[1] R. Alur and G. Weiss. Regular specifications of resource requirements for embedded control software. In *Proceedings of the 14th IEEE Real-time and Embedded Technology and Applications*, 2008.

[2] R. Alur and G. Weiss. RTComposer: a framework for real-time components with scheduling interfaces. In *Proceedings of the 8th ACM international conference on Embedded software*, pages 159–168. ACM, 2008.

[3] K.-E. Arzén, A. Cervin, J. Eker, and L. Sha. An introduction to control and scheduling co-design. In *Decision and Control, 2000. Proceedings of the 39th IEEE Conference on*, volume 5, pages 4865–4870. IEEE, 2000.

[4] K. J. Åström and T. Hägglund. *Advanced PID control*. ISA-The Instrumentation, Systems and Automation Society, 2006.

[5] J. Auerbach, D. F. Bacon, D. T. Iercan, C. M. Kirsch, V. T. Rajan, H. Roeck, and R. Trummer. Java takes flight: time-portable real-time programming with exotasks. In *Proceedings of the conference on Languages, Compilers, and Tools for Embedded Systems*, pages 51–62, 2007.

[6] A. Chakrabarti, L. de Alfaro, T. Henzinger, and M. Stoelinga. Resource interfaces. In *Embedded Software, 3rd International Conference*, LNCS 2855, pages 117–133, 2003.

[7] A. K. Das, R. Fierro, V. Kumar, J. P. Ostrowski, J. Spletzer, and C. J. Taylor. A vision-based formation control framework. *IEEE transactions on robotics and automation*, 18(5):813–825, 2002.

[8] L. de Alfaro and T. Henzinger. Interface automata. In *Proceedings of the Ninth Annual Symposium on Foundations of Software Engineering (FSE)*, pages 109–120. ACM Press, 2001.

[9] H. Efraim, S. Arogeti, A. Shapiro, and G. Weiss. Vision based output feedback control of micro aerial vehicles in indoor environments. *Journal of Intelligent & Robotic Systems*, 87(1):169–186, Jul 2017.

[10] E. Farcas, C. Farcas, W. Pree, and J. Templ. Transparent distribution of real-time components based on logical execution time. In *Proceedings of the conference on Languages, Compilers, and Tools for Embedded Systems*, pages 31–39, 2005.

[11] T. Henzinger and J. Sifakis. The embedded systems design challenge. In *FM 2006: 14th International Symposium on Formal Methods*, LNCS 4085, pages 1–15, 2006.

[12] T. A. Henzinger, B. Horowitz, and C. M. Kirsch.

Giotto: a time-triggered language for embedded programming. *Proceedings of the IEEE*, 91(1):84–99, 2003.

[13] W. T. Higgins. A comparison of complementary and kalman filtering. *IEEE Transactions on Aerospace and Electronic Systems*, (3):321–325, 1975.

[14] E. Lee. What's ahead for embedded software. *IEEE Computer*, pages 18–26, September 2000.

[15] E. A. Lee. Cyber physical systems: Design challenges. In *Object oriented real-time distributed computing (isorc), 2008 11th ieee international symposium on*, pages 363–369. IEEE, 2008.

[16] A. Mok and A. Feng. Towards compositionality in real-time resource partitioning based on regularity bounds. In *Proceedings of the 22nd IEEE Real-Time Systems Symposium*, pages 129–138, 2001.

[17] J. Regehr and J. Stankovic. HLS: A framework for composing soft real-time schedulers. In *Proceedings of the 22nd IEEE Real-Time Systems Symposium*, pages 3–14, 2001.

[18] A. Sangiovanni-Vincetelli, L. Carloni, F. D. Bernardinis, and M. Sgori. Benefits and challenges for platform-based design. In *Proceedings of the 41th ACM Design Automation Conference*, pages 409–414, 2004.

[19] S. Sastry, J. Sztipanovits, R. Bajcsy, and H. Gill. Modeling and design of embedded software. *Proceedings of the IEEE*, 91(1), 2003.

[20] O. Shakernia, Y. Ma, T. J. Koo, and S. Sastry. Landing an unmanned air vehicle: Vision based motion estimation and nonlinear control. *Asian journal of control*, 1(3):128–145, 1999.

[21] I. Shin and I. Lee. Compositional real-time scheduling framework with periodic model. *Trans. on Embedded Computing Sys.*, 7(3):1–39, 2008.

[22] P. Tabuada. Event-triggered real-time scheduling of stabilizing control tasks. *IEEE Transactions on Automatic Control*, 52(9):1680–1685, 2007.

[23] L. Thiele, E. Wanderer, and N. Stoimenov. Real-time interfaces for composing real-time systems. In *Proceedings of the 6th ACM/IEEE International Conference on Embedded Software*, pages 34–43, 2006.

[24] G. Weiss and R. Alur. Automata based interfaces for control and scheduling. In *International Workshop on Hybrid Systems: Computation and Control*, pages 601–613. Springer, 2007.

[25] G. Weiss and R. Alur. Automata based interfaces for control and scheduling. In *Proceedings of the 10th workshop on Hybrid Systems: Computation and Control*, 2007.

APPENDIX

Appendix goes here.